Carcinogenesis, 2020, Vol. 41, No. 8, 1145–1157

doi:10.1093/carcin/bgz193
Advance Access Publication December 5, 2019
Original Article

ORIGINAL ARTICLE

Recruitment of miR-8080 by luteolin inhibits androgen receptor splice variant 7 expression in castration-resistant prostate cancer

Aya Naiki-Ito[1,2,*], Taku Naiki[1,3], Hiroyuki Kato[1], Keitaro Iida[1,3], Toshiki Etani[3], Yuko Nagayasu[1], Shugo Suzuki[1], Yoriko Yamashita[1], Shingo Inaguma[1,2], Masaya Onishi[4], Yasuhito Tanaka[4], Takahiro Yasui[3] and Satoru Takahashi[1]

[1]Department of Experimental Pathology and Tumor Biology, Nagoya City University Graduate School of Medical Sciences, Nagoya 467-8601, Japan, [2]Pathology Division, Nagoya City East Medical Center, Nagoya 464-8547, Japan, [3]Department of Nephro-urology and [4]Department of Virology and Liver Unit, Nagoya City University Graduate School of Medical Sciences, Nagoya 467-8601, Japan

*To whom correspondence should be addressed. Department of Experimental Pathology and Tumor Biology, Nagoya City University Graduate School of Medical Sciences, 1-Kawasumi, Mizuho-cho, Mizuho-ku 467-8601, Nagoya, Japan. Tel: +81 52 853 8156; Fax: +81 52 842 0817; Email: ayaito@med.nagoya-cu.ac.jp
Correspondence may also be addressed to Satoru Takahashi, Department of Experimental Pathology and Tumor Biology, Nagoya City University Graduate School of Medical Sciences, 1-Kawasumi, Mizuho-cho, Mizuho-ku 467-8601, Nagoya, Japan. Tel: +81 52 853 8156; Fax: +81 52 842 0817; Email: sattak@med.nagoya-cu.ac.jp

Abstract

A need exists for seeking effective treatments for castration-resistant prostate cancer (CRPC) in response to its emergence following androgen deprivation therapy as a major clinical problem. In the present study, we investigated the chemopreventive and chemotherapeutic potential of luteolin, a flavonoid with antioxidative properties, on prostate cancer, including CRPC. Luteolin inhibited the progression of rat prostate carcinogenesis by induction of apoptosis in a transgenic rat for adenocarcinoma of prostate (TRAP) model. Luteolin decreased cell proliferation in a dose-dependent manner and induced apoptosis with the activation of caspases 3 and 7 in both rat (PCai1, established from a TRAP prostate tumor) and human (22Rv1) CRPC cells. Dietary luteolin also suppressed tumor growth via an increase in apoptosis and inhibition of angiogenesis in PCai1 and 22Rv1 xenografts implanted in castrated nude mice. We also focused on androgen receptor splice variant 7 (AR-V7), which contributes to cell proliferation and therapeutic resistance in CRPC. Luteolin dramatically suppressed AR-V7 protein expression in 22Rv1 cells *in vitro* and *ex vivo*. Microarray analysis identified *MiR-8080*, which contains a possible target sequence for AR-V7 3′-UTR, as a gene upregulated by luteolin. MiR-8080 transfection decreased the AR-V7 expression level and the induction of apoptosis in 22Rv1 cells. Furthermore, miR-8080 knockdown canceled luteolin decreasing AR-V7 and the cell growth of 22Rv1. MiR-8080 induced by luteolin intake enhanced the therapeutic effect of enzalutamide on 22Rv1 xenografts under castration conditions. These results indicate luteolin inhibits CRPC by AR-V7 suppression through miR-8080, highlighting luteolin and miR-8080 as promising therapeutic agents for this disease.

Introduction

Prostate cancer is the most common noncutaneous malignancy in the United States and is responsible for many male deaths in 2018, second only to lung cancer (1). Though the incidence and mortality rate for prostate cancer are lower in Japan as compared with Western countries, these have dramatically increased. Environmental factors, including dietary habits and

Received: January 22, 2019; **Revised:** October 28, 2019; **Accepted:** November 22, 2019

Abbreviations

AR	androgen receptor
AR-FL	full-length androgen receptor
AR-V7	androgen receptor splice variant 7
AR-Vs	spliced variants of the AR
CRPC	castration-resistant prostate cancer
DCFH-DA	dichloro-dihydro-fluorescein diacetate
ER	endoplasmic reticulum
FBS	fetal bovine serum
IGF-1R	insulin-like growth factor-1 receptor
luteolin	3′,4′,5,7-tetrahydroxy flavone
NASH	nonalcoholic steatohepatitis
PIN	prostatic intraepithelial neoplasia
ROS	reactive oxygen species
TRAP	transgenic rat for adenocarcinoma of prostate

lifestyle, account for the observed increase in prostate cancer. For instance, epidemiological evidence and animal studies indicate that red meat and fat in the diet are possible risk factors for prostate cancer (2–4). They promote carcinogenesis by affecting oxidative stress, cell proliferation and apoptosis (5). Therefore, a dietary intake of antioxidants may an effective intervention for preventing prostate cancer.

Various fruits, vegetables, tea and other foods derived from plant sources contain an abundance of natural antioxidants. Major components include carotenoids, vitamin E and polyphenols, including flavonoids. As we have previously reported, such antioxidants prevent prostate carcinogenesis (6–9). Luteolin (3′,4′,5,7-tetrahydroxy flavone) is a flavonoid with anti-inflammatory and antioxidative properties that is present in perilla seeds, celery, green pepper and parsley (10). Luteolin is also known as an anticancer agent in various cancers, including those of the colon, liver and breast. Luteolin downregulates insulin-like growth factor-1 receptor (IGF-1R) signaling, and induces cell-cycle arrest and apoptosis in the colon cancer cell line, HT-29 (11). Another study reported that luteolin inhibits chemical-induced colon carcinogenesis in rats (12,13). In addition, recent experiments by us indicate that a dietary luteolin intake prevents steatohepatitis and the production of hepatic preneoplastic foci by reducing reactive oxygen species (ROS) in a methionine–choline deficient diet-induced rat nonalcoholic steatohepatitis model (14). This evidence suggests that luteolin has a chemopreventive potential for early carcinogenesis. However, the effect of luteolin on the development of prostate cancer has not been investigated.

The development of prostate carcinogenesis is initially androgen-dependent (15). However, the progression of castration-resistant prostate cancer (CRPC) following androgen deprivation therapy is a major clinical problem. Although enzalutamide and abiraterone have been approved for CRPC hormone therapy (16,17), and several new drugs are under development, including EPI-002 and galeterone (18,19), the efficacy of these drugs is limited. Besides the mutation and amplification of the androgen receptor (AR), spliced variants of the AR (AR-Vs) protein, such as AR splice variant 7 (AR-V7) which lacks a functional ligand-binding domain, stand out as a major resistance mechanism in CRPC (20).

In this study, we investigated the antioxidative and chemopreventive effect of luteolin on prostate carcinogenesis using a transgenic rat for adenocarcinoma of prostate (TRAP) model (21,22). Moreover, luteolin has been highlighted as a therapeutic agent in a rat CRPC tumor model (23,24). The inhibitory effect of luteolin on AR-V7 was a major factor in its therapeutic effect against CRPC. Finally, we identified the recruitment of miR-8080 expression as directly reducing AR-V7 expression.

Materials and methods

Chemicals

Luteolin was purchased from Tokyo Kasei Kogyo Co. Ltd (Tokyo, Japan). Enzalutamide (MDV3100) was obtained from Selleck Chemicals (Houston, TX).

Prostate cancer cell lines

Human prostate cancer cell lines, 22Rv1 and VCaP, were obtained from the American Tissue Culture Collection (Rockville, MD). All cells were authenticated by short tandem repeat profiling before receipt and were propagated for less than 6 months after resuscitation. Additionally, PCai1, a CRPC cell line originally established from a rat TRAP tumor, was cultured as described previously (24,25).

Animals

All experimental rats or mice were housed three or four per plastic cage on wood-chip bedding in an air-conditioned specific pathogen-free animal room at 22 ± 2°C and 55 ± 5% humidity with a 12-h light/dark cycle. Food and tap water were available *ad libitum*. The present experiments were performed under protocols approved by the Institutional Animal Care and Use Committee of Nagoya City University School of Medical Sciences.

Animal experiments for chemopreventive analysis

Heterozygous male TRAP rats with a Sprague–Dawley genetic background used in this study were established in our laboratory, as described previously (21). A total of 36 male TRAP rats at 6 weeks of age were randomly divided into three groups. Rats in the control group (n = 12) received a basal diet (AIN-76A; Oriental Bio Service, Kyoto, Japan) and tap water. Rats in the other two groups continuously received either 20 or 100 ppm luteolin in their diet for 8 weeks. Samples including prostate lobes were collected as described previously (26).

Animal experiments for chemotherapeutic evaluation

PCai1 cells were subcutaneously implanted into castrated male nude mice as described previously (24,25). A total of 45 mice were randomly divided into control, 20 or 100 ppm luteolin groups, with luteolin received from diets. Body weights and tumor volumes were calculated every week, and mice were killed at 6 weeks. Cells (22Rv1, 1×10^6) in 100 µL of RPMI1640 (Thermo Fisher Scientific, Rockford, IL) were mixed with Matrigel and subcutaneously implanted into castrated nude mice. A total of 40 mice were randomly divided into control or 100 ppm of luteolin groups, with luteolin received from diets. Body weights and tumor volumes were calculated every week, and mice killed at 4 weeks. Tumor volumes were calculated using the formula, $V = (A \times B^2)/2$, where V represents volume in mm^3, and A and B represent long and short diameters in mm, respectively.

Animal experiments for combined administration of luteolin and enzalutamide

Forty-eight 22Rv1 xenograft tumors were prepared as described above. When tumors reached 25 mm^3, mice were randomized into four groups for daily treatment: (i) vehicle (saline with 21% PGE300, 3.75% dimethyl sulfoxide intraperitoneally [i.p.] injected 5 times weekly); (ii) enzalutamide (10 mg/kg/day, suspended in saline with 21% PGE300, 3.75% dimethyl sulfoxide i.p. injected 5 times weekly); (iii) luteolin (100 ppm received from the diet); and (iv) enzalutamide plus luteolin (combination). Mice were weighed and tumor volumes measured every other day for 2 weeks.

Assessment of prostate neoplastic lesion development

Neoplastic lesions of the prostate gland were classified as low-grade prostatic intraepithelial neoplasia (LG-PIN), high-grade PIN (HG-PIN) or

noninvasive adenocarcinoma, as described previously (7,26). The number of LG-PIN, HG-PIN, and adenocarcinoma lesions in the ventral prostate (VP) and lateral prostate (LP) was scored blindly by two experts in diagnostic pathology (A.N-I. and S.T.) and presented as a percentage of lesions in each prostate.

Detection of ROS production

Frozen prostate sections from 10 rats in each group were cut to a 6-μm thickness and incubated with 5 μM dihydroethidium (Thermo Fisher Scientific) in phosphate buffered saline for 15 min in the dark to detect ROS. The slides were washed with phosphate buffered saline and assessed at 518/605 nm with an image analyzer (BZ-9000 fluorescence microscope; Keyence, Osaka, Japan). Five images per rat were taken at random with the same exposure time at ×400 magnification, and then the average fluorescence intensity in the nucleus of HG-PIN was quantified using software (BZ-analysis application, Keyence).

Cell viability assay

Cell viability was analyzed by WST-1 cell proliferation assay (Roche Diagnostic, Basel, Switzerland) as described previously (8). Cells were seeded in 96-well plates at 1×10^4 cells per well. Each treatment was performed 24 h after seeding and cells incubated for 48 h. Apoptotic cells were stained by ViaCount Assay (Merck, Darmstadt, Germany) and counted on Guava® Flow Cytometers (Merck).

Measurement of intracellular ROS level *in vitro*

For the measurement of the intracellular ROS level in 22Rv1 and PCai1 cells, a dichloro-dihydro-fluorescein diacetate assay (Thermo Fisher Scientific) was performed as described previously (24).

Quantitative reverse transcription–polymerase chain reaction

One microgram of RNA was converted to cDNA with avian myoblastosis virus reverse transcriptase (Takara, Otsu, Japan) in 20 μl reaction mixture. Aliquots of 2 μl of cDNA samples were subjected to quantitative polymerase chain reaction in a total volume of 25 μl using SYBR Premix ExTaq II (Takara) in a light cycler apparatus (Roche Diagnostic Basel). The primers used are listed in Supplementary Table S1, available at *Carcinogenesis* Online. Glyceraldehyde 3-phosphate dehydrogenase mRNA levels were used as internal controls.

RNA interference

Specific siRNAs for full-length androgen receptor (AR-FL) (target sequence: UCAAGGAACUCGAUCGUAU) and AR-V7 (target sequence: GUAGUUGUGAGUAUCAUGA) were synthesized by Sigma–Aldrich (St. Louis, MO) and used for gene silencing (27). Cells (1×10^5 22Rv1) were seeded into 6-well plates and transfected with siRNA at a final concentration of 40 nM using Lipofectamine RNAiMAX (Thermo Fisher Scientific) according to the manufacturer's instructions.

Microarray analysis

Gene expression analysis was performed using a Human Oligo chip 25k (Toray Industries, Tokyo, Japan) for DNA microanalysis and a Human miRNA V21 chip (Toray Industries) for microRNA (miRNA) according to the manufacturer's instructions. Gene expression was compared between 22Rv1 cells treated with or without 25 μM luteolin for 48 h. The original microarray data are available in a Gene Expression Omnibus database repository submission (GSE126856 and GSE120181).

Quantitative reverse transcription–polymerase chain reaction for miRNA

Using a TaqMan MiRNA Reverse Transcription Kit, cDNA was synthesized to detect miR-8080 (Thermo Fisher Scientific) in reverse transcription–polymerase chain reaction. Relative miR-8080 expression was detected using TaqMan® Gene Expression Assays (Thermo Fisher Scientific) on an AriaMx Real-Time PCR System (Agilent Technologies, Santa Clara, CA). Expression ratios were calculated as the normalized Ct difference between the control and sample and were adjusted for amplification efficiency relative to the expression level of the housekeeping gene, *RNU6B*.

Transfection of miRNA expression vector and miRNA inhibitor

Expression (miR-8080) and empty (pCMV-MIR) vectors were purchased from ORIGENE (Rockville, MD). An miR-8080 inhibitor and miRNA negative control were synthesized by Thermo Fisher Scientific. The expression vector (miR-8080) or inhibitor was transfected into 22Rv1 cells using Lipofectamine 3000 (Thermo Fisher Scientific) according to the manufacturer's instructions.

Western blotting analyses

Prostate cancer cells or frozen tissues were homogenized with Radio-Immunoprecipitation Assay buffer (Thermo Fisher Scientific) containing protease and phosphatase inhibitors (Thermo Fisher Scientific). Protein concentrations were quantified by the Bradford procedure and equal amounts of proteins used as samples. Samples were loaded at 30 μg per lane, separated on acrylamide gels and electroblotted onto nitrocellulose membranes (Hybond-ECL; GE Healthcare UK Ltd, Buckinghamshire, UK). The primary antibodies used in this study were against: caspase 3, caspase 7, cleaved (cl)-caspase 3, cl-caspase 7, nuclear factor-κB, pNF-κB (Ser536), cyclin D1 (Cell Signaling, Boston, MA); AR (N-20, N-terminus), SV-40 T antigen (Santa Cruz Biotechnology, Dallas, TX) and AR-V7 (Abcam, Cambridge, UK). Equal protein loading was ascertained by western blotting with β-actin antibody (Sigma–Aldrich). The intensity of each band was measured using Image *J* software program, ver. 1.46 (National Cancer Institute, Bethesda, MD).

Immunohistochemistry

Deparaffinized sections were incubated with antibodies against AR (Santa Cruz Biotechnology), SV40 T antigen (Santa Cruz Biotechnology), Ki-67 (Novocastra Laboratories Ltd, Newcastle, UK), GPX2 (Medical & Biological Laboratories Co., Ltd, Ina, Nagoya, Japan), CD31 (Abcam) and AR-V7 (GeneTex, Irvine, CA). Apoptotic cells were detected by a terminal deoxy nucleotidyl transferase-mediated dUTP nick end labeling (TUNEL) assay. The TUNEL assay was performed using an *in situ* Apoptosis Detection Kit from Takara. The labeling indices of Ki-67 and TUNEL were determined by counting at least 1000 HG-PIN cells under a microscope at high magnification.

MG132 treatment

22Rv1 cells were seeded into 6-well plates and incubated for 24 h. Cells were treated with 25 μM luteolin and/or 5 μM MG132 for 16 h, and then lysed with Radio-Immunoprecipitation Assay buffer supplemented with protease inhibitor cocktail (Thermo Fisher Scientific).

Statistical analysis

Differences in quantitative data, which are expressed as mean ± standard deviation, between groups were compared by one-way analysis of variance and Dunnett's *post hoc* test using GraphPad Prism 5 (GraphPad Software, La Jolla, CA). A P-value <0.05 was considered significant.

Results

Luteolin suppresses rat prostate carcinogenesis in a TRAP model via the induction of apoptosis and inhibition of cell proliferation

Luteolin intake did not affect body weight or weights of the liver, kidneys or the VP (Supplementary Table S2, available at *Carcinogenesis* Online). Serum testosterone levels were significantly elevated by luteolin in a dose-dependent manner (Supplementary Table S2, available at *Carcinogenesis* Online). However, a significant difference in the testosterone/estradiol (T/E2) ratio among rat groups was not noted (Supplementary Table S2, available at *Carcinogenesis* Online). Histological analysis

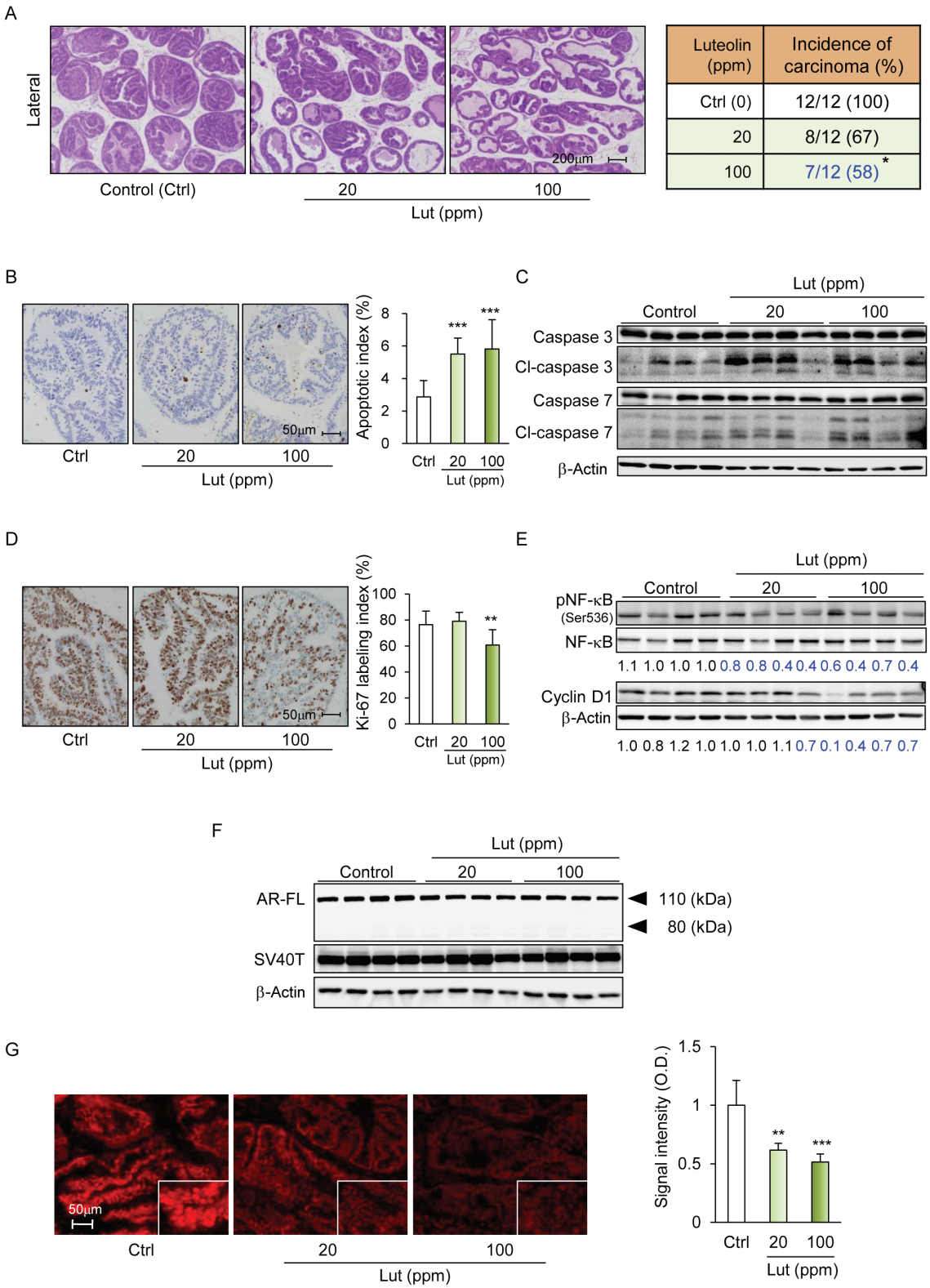

Luteolin (ppm)	Incidence of carcinoma (%)
Ctrl (0)	12/12 (100)
20	8/12 (67)
100	7/12 (58)*

Figure 1. Attenuation effect of luteolin in prostate carcinogenesis using TRAP model. (**A**) Representative histological findings of the LP of TRAP rats from control (Ctrl) and luteolin (Lut; 20, 100 ppm) treated groups. The incidence of adenocarcinoma in the LP from rats treated with luteolin. $n = 12$ per group, $^{*}P < 0.05$ statistically significant as compared with control group. (**B**) The labeling indices for TUNEL-positive cells in the LP for each treatment. Data are presented as the mean ± SD, $n = 12$ per group, $^{***}P < 0.001$ statistically significant as compared with control group. (**C**) Western blotting analyses for caspases 3 and 7, and cl-caspases 3 and 7 in the LP. β-Actin was used as an internal loading control. (**D**) The labeling index for Ki-67-positive cells in the LP of rats from each treatment. Data are presented as the mean ± SD, $n = 12$ per group, $^{**}P < 0.01$ statistically significant as compared with control group. (**E**) Western blotting analyses for phosphorylated nuclear factor-κB and cyclin D1 in the LP. (**F**) Western blotting analyses for AR-FL and SV40T in the LP. β-Actin was used as an internal loading control. (**G**) Representative DHE staining for the detection of intracellular ROS levels in the LP. The signal intensity of DHE staining was presented as the mean ± SD, $^{**}P < 0.01$, $^{***}P < 0.001$ statistically significant as compared with control group.

revealed that luteolin treatment significantly suppressed the progression of prostatic lesions from LG-PIN to HG-PIN or adenocarcinoma in both the VP and LP of TRAP rats (Supplementary Table S3, available at *Carcinogenesis* Online, Figure 1A, and Supplementary Figure S1A, available at *Carcinogenesis* Online). In both the VP and LP, the percentage of LG-PIN lesions was significantly increased and the percentage of adenocarcinomas was significantly decreased by luteolin. Furthermore, the incidence of adenocarcinoma in the LP was significantly decreased by treatment with a high dose of luteolin when compared with control.

To determine the effects of luteolin on cell proliferation or apoptosis during prostate carcinogenesis, Ki-67 and TUNEL labeling indices, respectively, in HG-PIN lesions among each group were evaluated. Apoptotic indices were significantly increased in a dose-dependent manner in the VP and LP of TRAP rats treated with luteolin as compared with control (Figure 1B; $P < 0.001$ and Supplementary Figure S1B, available at *Carcinogenesis* Online). The Ki-67 labeling index was decreased by luteolin in both the VP and LP (Figure 1D; $P < 0.01$ and Supplementary Figure S1C, available at *Carcinogenesis* Online). Western blotting analyses revealed the activation of caspases 3 and 7 in the VP and LP of TRAP rats treated with luteolin; phosphorylated nuclear factor-κB and cyclin D1 expression was slightly decreased by luteolin treatment (Figure 1C, E and Supplementary Figure S1D, available at *Carcinogenesis* Online). We confirmed that luteolin did not affect AR and SV40 T expression in TRAP rats (Figure 1F, Supplementary Figures S1D and S2, available at *Carcinogenesis* Online). Further, we demonstrated by immunoblotting that AR-Vs were not expressed in this model (Figure 1F and Supplementary Figure S1D, available at *Carcinogenesis* Online). These results indicated that luteolin suppresses the development of prostate carcinogenesis via the induction of caspase-dependent apoptosis.

Luteolin decreases oxidative stress in prostate of the TRAP model

We previously confirmed the ability of luteolin to prevent the accumulation of hepatic ROS during nonalcoholic steatohepatitis development (14). Therefore, we next investigated any alteration of oxidative stress levels during the development of prostate carcinogenesis in our TRAP model and the effect of luteolin. Dihydroethidium staining assays indicated that the level of ROS was increased in adenocarcinoma and HG-PIN as compared with LG-PIN. As was the case in nonalcoholic steatohepatitis, dietary luteolin significantly suppressed the production of ROS in HG-PIN in a dose-dependent manner (Figure 1G; $P < 0.001$). The mRNA expression of the oxidative stress-related genes, *Gpx2*, *clusterin*, *Ho-1* and *Il-1b*, was significantly downregulated by luteolin (Supplementary Figure S3A, available at *Carcinogenesis* Online). Western blot confirmed the decrease of Gpx2 and clusterin protein expression in the VP of TRAP rats with luteolin treatment (Supplementary Figure S3B, available at *Carcinogenesis* Online).

Luteolin inhibits cell proliferation and induces apoptosis in rat CRPC cells both *in vitro* and *ex vivo*

Gpx2 is a key enzyme of the glutathione redox system and has an antioxidant function; its expression was decreased by luteolin intake in the TRAP prostate. We previously found that the *Gpx2* gene was responsible for mammary carcinogenesis in both rats and human (28). Moreover, Gpx2 is involved in the proliferation and prognosis of cancers, including CRPC and those of the liver and urinary bladder (25,29,30). This accumulated evidence led us to investigate the possible roles of luteolin in CRPC. We investigated whether luteolin affected the cell proliferation of the rat CRPC cell line, PCai1. Luteolin significantly suppressed the cell viability of PCai1 cells in a dose-dependent manner in the presence of both normal fetal bovine serum (FBS) and charcoal-stripped–FBS (Figure 2A; $P < 0.001$). Luteolin significantly decreased the production of ROS ($P < 0.001$), and significantly increased the percentage of apoptotic cells ($P < 0.05$), as well as the expression of cleaved caspases 3 and 7 (cl-caspases 3 and 7) under both conditions (Figure 2B–D and Supplementary Figure S4, available at *Carcinogenesis* Online). PCai1 cells expressed AR-FL but no AR-Vs in common with its original TRAP tumor; this was confirmed by RNA sequencing (data not shown). AR-FL was not affected by luteolin (Figure 2D). To evaluate the effect of dietary luteolin on CRPC tumors, castrated nude mice with subcutaneously transplanted PCai1 cells were fed luteolin for 6 weeks. Luteolin treatment significantly inhibited the growth of CRPC tumors using both doses of 20 and 100 ppm (Figure 2E; $P < 0.01$). Luteolin treatment significantly increased the percentage of TUNEL-positive apoptotic cells ($P < 0.001$), and decreased the expression of Gpx2 ($P < 0.001$) and vessel density ($P < 0.05$) as compared with control (Figure 2F–H). Both *in vitro* and *ex vivo* data suggested that luteolin worked as an antioxidant and induces apoptosis in CRPC tumors, as was observed in early prostate carcinogenesis.

Luteolin inhibits cell proliferation and AR-V7 expression in human CRPC cells

In accordance with the suppressive effect of luteolin on rat CRPC, we were interested in the effect of luteolin on the expression of AR-V7, which is involved in the pathogenesis and drug resistance of CRPC. Cell viability was significantly inhibited by luteolin treatment in a dose-dependent manner ($P < 0.001$); a significant decrease in the ROS level was also observed (Figure 3A and B; $P < 0.05$). The growth inhibition of cultured CRPC cells by luteolin was observed in the presence of charcoal-stripped–FBS (Figure 3A). To determine the effect of luteolin on AR-V7 expression, the expression status was measured in LNCaP, 22Rv1 and VCaP cell lines. The expression of AR-FL mRNA in VCaP, and AR-V7 mRNA in 22Rv1 and VCaP cell lines was high. Strong protein expression of AR-FL and AR-V7 was also detected in 22Rv1 and VCaP cells (Figure 3C). Significant changes in AR-FL mRNA expression by luteolin were not observed (Figure 3D). However, AR-V7 mRNA expression was significantly decreased by luteolin in 22Rv1 cells (Figure 3D; $P < 0.01$, $P < 0.001$). Among other AR-Vs, AR-V9 mRNA expression was reduced by luteolin in a dose-dependent manner (Figure 3D; $P < 0.01$, $P < 0.001$), while luteolin had no dose-dependent effect on other AR-Vs. AR-V9 is frequently co-expressed with AR-V7 in 22Rv1 cells and clinical CRPC (31,32). Interestingly AR-V7 and AR-V9 shared a common 3′-terminal crypt exon, CE3, which was shown previously to uniquely target AR-V7. Furthermore, CE3-targeted RNAi knocked-down not only AR-V7, but also AR-V9 (32). Overall, these data indicated that the inhibitory effect of luteolin on AR-Vs was exon CE3-dependent. Western blotting analysis revealed that luteolin dramatically decreased AR-V7 expression, while it slightly decreased AR-FL (Figure 3E). Activation of caspases 3 and 7, and suppression of Gpx2 were induced by luteolin (Figure 3E). Similar significantly suppressive effects on cell proliferation ($P < 0.001$), decreased expression of AR-V7, and the elevation of cl-caspases were also observed in VCaP and 22Rv1 cells with charcoal-stripped–FBS (Figure 3F and G). Knockdown of AR-FL or AR-V7 was accompanied by decreased cell proliferation in

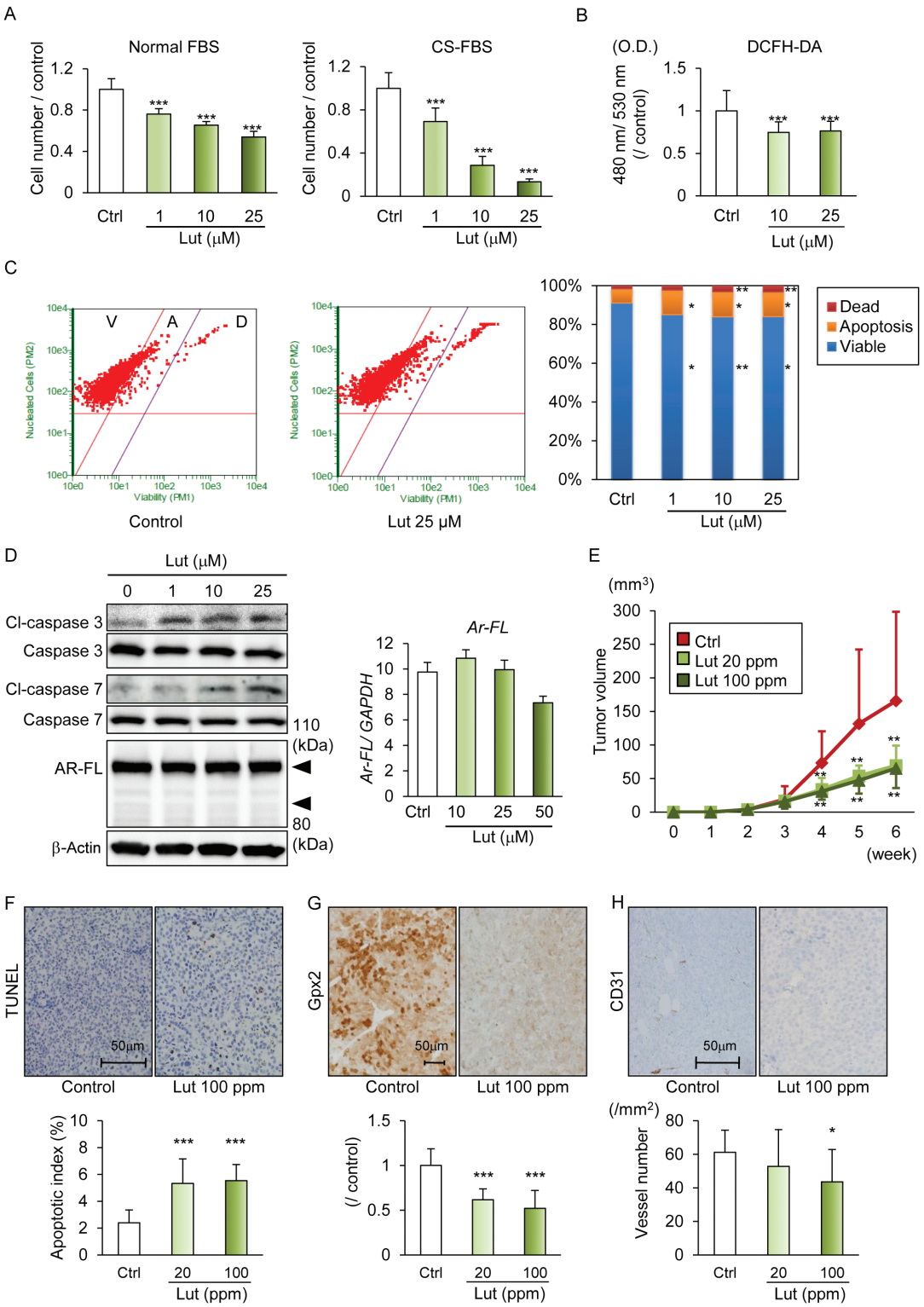

Figure 2. Therapeutic effect of luteolin on rat CRPC cell line, PCai1, *in vitro* and *ex vivo*. (**A**) The proliferation rate of PCai1 cells at 5 days following luteolin (Lut) treatment with normal FBS (left) and CS–FBS medium (right). Data are presented as mean ± SD, $n = 5$ per group, ***$P < 0.001$ statistically significant as compared with control (Ctrl) group. (**B**) Intracellular ROS level in PCai1 cells by dichloro-dihydro-fluorescein diacetate assay (480 nm/530 nm). O.D., optical density. Data are presented as mean ± SD, $n = 24$ per group, ***$P < 0.001$ statistically significant compared with control group. (**C**) PCai1 cells treated with luteolin for 48 h and stained with Guava® ViaCount to separate viable (V), apoptotic (A) or dead (D) cells. The survival status after each treatment is presented in the bar chart, $n = 5$, *$P < 0.05$, **$P < 0.01$ statistically significant compared with control group. (**D**) Western blotting analyses for caspases 3 and 7, cl-caspases 3 and 7, AR-FL or β-actin in PCai1 cells. The AR-FL mRNA level was measured byquantitative reverse transcription–polymerase chain reaction. The primers used are listed in Supplementary Table S1, available at *Carcinogenesis* Online. Glyceraldehyde 3-phosphate dehydrogenase was used as an internal control. (**E**) Tumor volume of PCai1 xenografts (1.0×10^6) in castrated nude mice. Mice received a control diet or a diet with luteolin (20 or 100 ppm). Data are presented as mean ± SD, in each week. $n = 15$ per group, **$P < 0.01$ statistically significant compared with control group. (**F–H**) Representative TUNEL (F), Gpx2 (G) and vessel density by CD31 immunohistochemistry (H) staining in PCai1 xenografts in castrated nude mice. Data are presented as mean ± SD, $n = 15$, *$P < 0.05$, ***$P < 0.001$ statistically significant compared with control group.

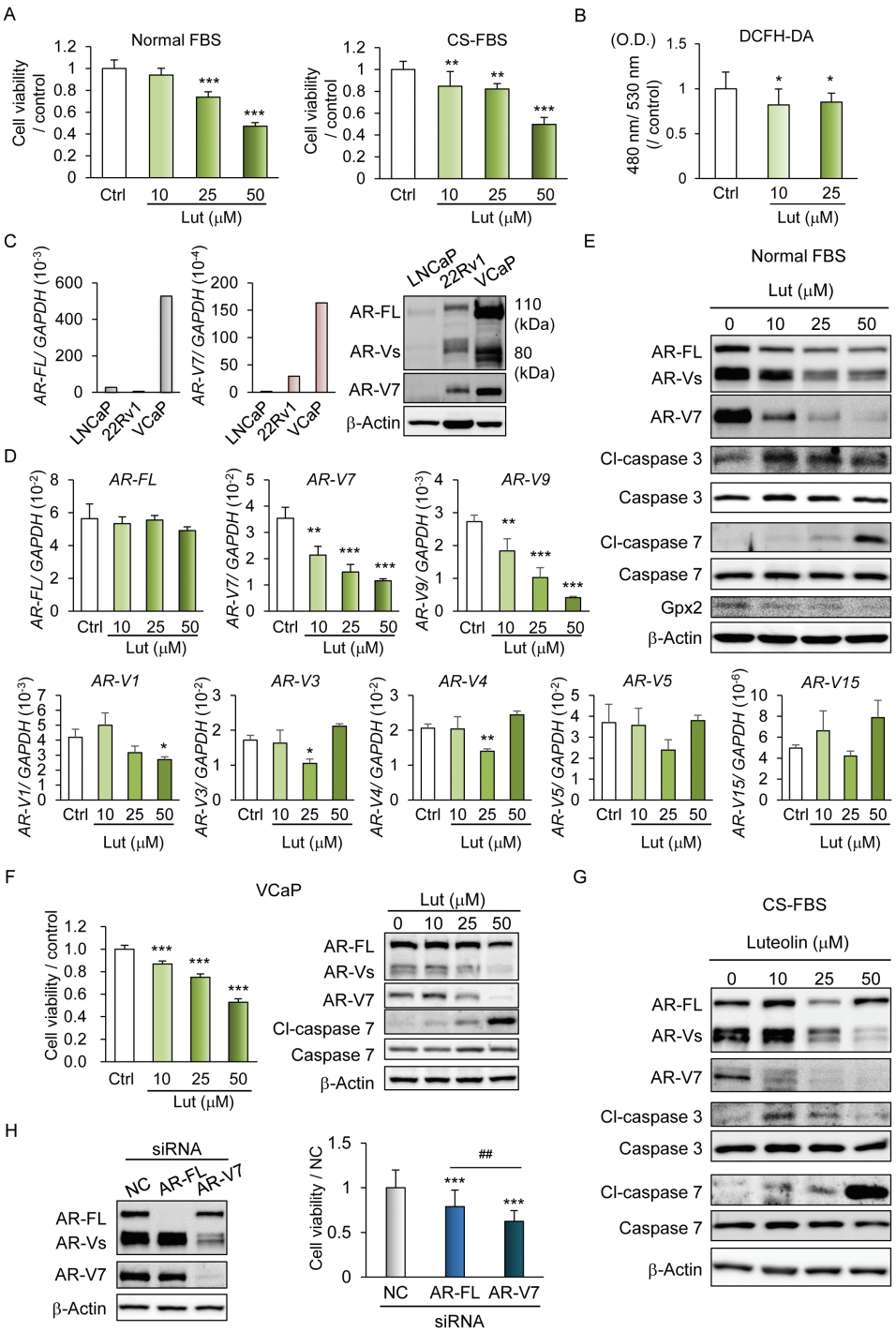

Figure 3. Suppressive effect of luteolin on cell proliferation by induction of caspase-dependent apoptosis via regulation of AR-V7 expression in human CRPC cell lines *in vitro*. (**A**) The proliferation rate of 22Rv1 cells after luteolin (Lut) treatment for 48 h with normal FBS (left) and CS–FBS medium (right). Data are presented as mean ± SD, $n = 4$ per group, $^{**}P < 0.01$, $^{***}P < 0.001$ statistically significant compared with control (Ctrl) group. (**B**) Intracellular ROS level in 22Rv1 cells by dichloro-dihydro-fluorescein diacetate assay (480 nm/530 nm). O.D., optical density. Data are presented as mean ± SD, $n = 24$ per group, $^{*}P < 0.05$ statistically significant compared with control group. (**C**) The expression of AR-FL and AR-V7 expression in human prostate cancer cell lines, LNCaP, 22Rv1 and VCaP. The mRNA levels were measured by quantitative reverse transcription–polymerase chain reaction. The primers used are listed in Supplementary Table S1, available at *Carcinogenesis* Online. Glyceraldehyde 3-phosphate dehydrogenase was used as an internal control. Protein levels were assessed by western blotting analyses and AR antibody detected both AR-FL (110 kDa) and AR-Vs (80 kDa). β-Actin was used as an internal loading control. (**D**) The mRNA levels of AR-FL, AR-V7 and other AR-Vs in 22Rv1 cells treated with luteolin for 48 h were analyzed by quantitative reverse transcription–polymerase chain reaction. Data are presented as mean ± SD, $n = 4$ per group, $^{**}P < 0.01$, $^{***}P < 0.001$ statistically significant compared with control group. (**E**) Western blotting analyses for AR-FL, AR-V7, cl-caspases 3 and 7, caspases 3 and 7, Gpx2 and β-actin in 22Rv1 cells treated with luteolin for 48 h. (**F**) The proliferation rate in VCaP cells treated with luteolin for 48 h. Data are presented as mean ± SD, $n = 4$ per group, $^{***}P < 0.001$ statistically significant compared with control group. Western blotting analyses for AR-FL, AR-V7, cl-caspase 7, caspase 7 and β-actin in VCaP cells treated with luteolin for 48 h. (**G**) Western blotting analyses for AR-FL, AR-V7, cl-caspases 3 and 7, caspases 3 and 7, and β-actin in 22Rv1 cells in CS–FBS treated with luteolin for 48 h. (**H**) The 22Rv1 cell line was transfected with either negative control siRNA, AR-FL siRNA or AR-V7 siRNA. Western blotting analyses for AR-FL and AR-V7. Each proliferation rate is presented as mean ± SD, $n = 24$ per group, $^{***}P < 0.001$ statistically significant compared with control group. $^{\#\#}P < 0.01$ statistically significant between the groups shown.

22Rv1 cells (Figure 3H; $P < 0.001$ for both). The inhibitory effect on cell proliferation was significantly stronger after AR-V7 knockdown than by AR-FL knockdown (Figure 3H; $P < 0.01$).

Dietary luteolin suppresses CRPC tumor growth with apoptosis induction and AR-V7 downregulation

To investigate whether luteolin intake could inhibit the growth of CRPC tumors, we used a subcutaneously implanted 22Rv1 tumor model in castrated nude mice that were treated with luteolin. Tumor volume was significantly reduced in the luteolin group as compared with that of control group (Figure 4A; $P < 0.001$). Western blot analysis showed AR-FL and AR-V7 decreased after luteolin intake (Figure 4B). Immunohistochemistry for AR-V7 indicated that the AR-V7 protein was localized in nuclei and its labeling index was significantly suppressed by luteolin (Figure 4C; $P < 0.001$). As with PCai1 CRPC tumors, luteolin significantly

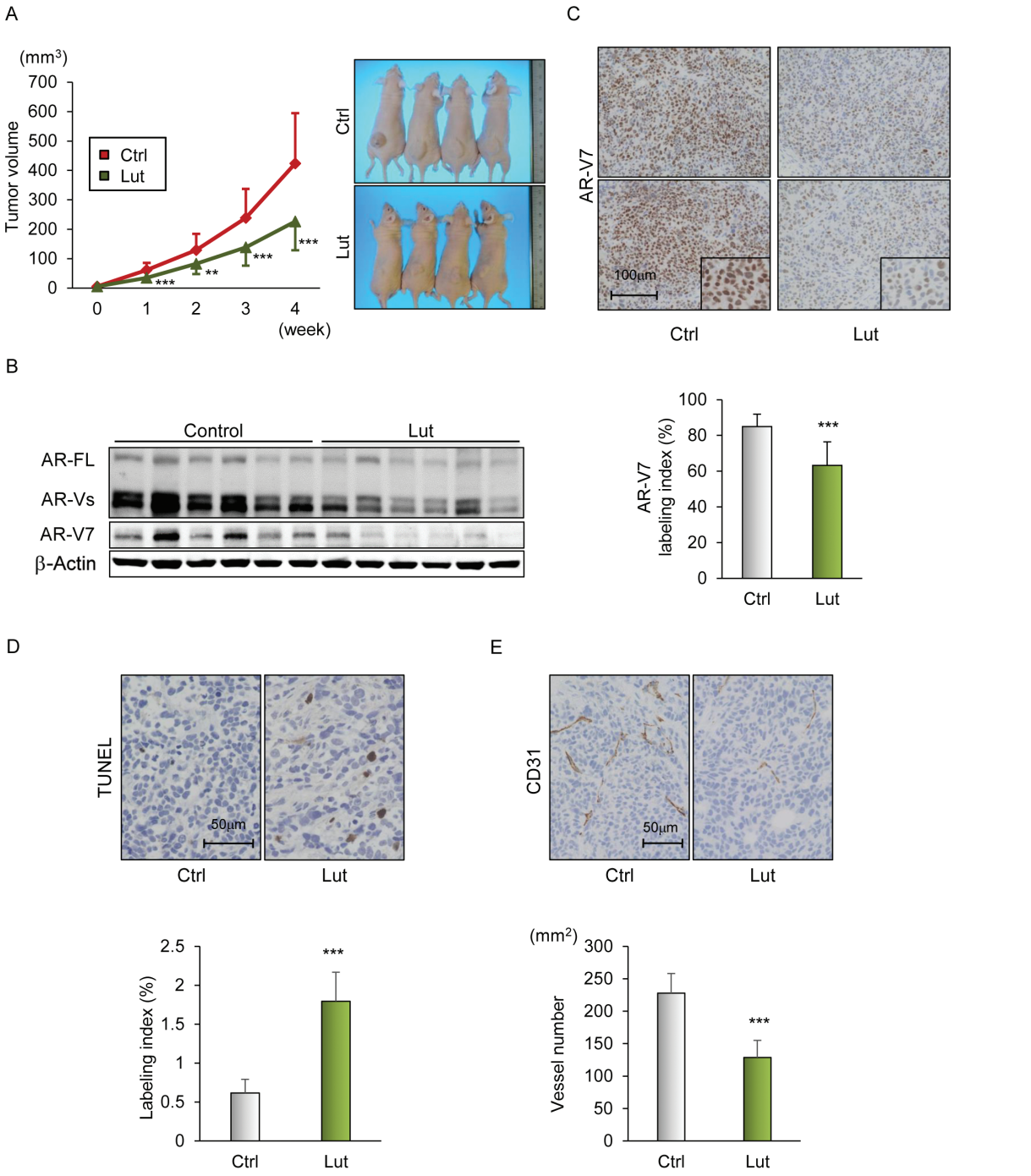

Figure 4. Therapeutic effect of luteolin on CRPC tumor growth by suppression of AR-V7 in a 22Rv1 xenograft model. (**A**) Tumor volume of 22Rv1 xenografts (1.0×10^6 cells) in castrated nude mice. Mice received a control diet (Ctrl) or a diet with luteolin (Lut; 20 or 100 ppm). Data are presented as mean ± SD, in each week. $n = 20$ per group, $^{**}P < 0.01$, $^{***}P < 0.001$ statistically significant compared with control group. Representative tumors in each group at 4 weeks after treatment. (**B**) Western blotting analyses for AR-FL, AR-V7 and β-actin in 22Rv1 xenografts. (**C–E**) The labeling indices for AR-V7 (C), TUNEL (D) and vessel density by CD31 immunohistochemistry (E) in 22Rv1 xenografts. Data are presented as mean ± SD, $n = 20$, $^{***}P < 0.001$ statistically significant compared with control group.

increased the rate of apoptosis and inhibited angiogenesis (Figure 4D and E; $P < 0.001$ for both). These results suggested that dietary luteolin controlled AR-FL and AR-V7 in CRPC tumors.

MiR-8080 is induced by luteolin and downregulates AR-V7 in CRPC

Because of the suppressive effect of luteolin on AR-V7 in CRPC cells *in vitro* and *in vivo*, we explored the mechanisms involved in the downregulation of AR-V7 by luteolin in CRPC. Based on the gap between mRNA and protein in the level of AR-V7 downregulation by luteolin, we hypothesized that post-translational regulatory mechanisms were important in the suppression of AR-V7 by luteolin. The suppressive effect of luteolin on AR-V7 protein expression was blocked by the proteasome inhibitor, MG132, suggesting that a proteasome-dependent pathway was involved in AR-V7 downregulation by luteolin (Figure 5A). Furthermore, we analyzed the modulation of AR-V7 through miRNA induction. To identify genes related to AR-V7 downregulation in CRPC, we measured changes in the expression of miRNAs by microarray analysis after luteolin treatment of 22Rv1 cells. The miRNAs that were upregulated more than 2-fold by luteolin, contained miRNAs targeting AR (e.g. miR-19a-3p, miR-301a-3p, miR-9-5p and miR-27b-3p) or insulin-like growth factor (IGF) 1 (e.g. miR-148a-3p, miR-19a-3p, miR-29b-3p and miR-148b-3p) (Supplementary Table S4, available at *Carcinogenesis* Online). The IGF-1R pathway, stimulated by IGF1, contributes to proliferation and chemoresistance in prostate cancer (33), including in a case of abiraterone treatment of CRPC (34). We performed *in silico* analysis using an miRBase Sequence Database to detect miRNAs that directly interact with AR-V7. Among miRNAs upregulated by luteolin, hsa-miR-8080 (Association ID: MIMAT0031007) was identified as a miRNA that is able to bind the 3′-untranslated region (3′-UTR) of AR-V7 (Figure 5B). Quantitative reverse transcription–polymerase chain reaction confirmed that miR-8080 was significantly upregulated by luteolin as compared with control in 22Rv1 cells (Figure 5C; $P < 0.05$). Interestingly, quercetin and apigenin, which are flavonoids and have a similar structure to luteolin (Supplementary Figure S5, available at *Carcinogenesis* Online), also significantly induced miR-8080 expression (Figure 5C; $P < 0.05$ for both). Inversely proportional to the miR-8080 level, the AR-V7 protein level were reduced by these flavonoids (Figure 5D). To clarify the direct interaction between miR-8080 and AR-V7, an miR-8080 expression vector was transfected into 22Rv1 cells. Forced transfection of miR-8080 caused a decrease in AR-V7 and significantly suppressed cell proliferation by the induction of caspase-dependent apoptosis (Figure 5E; $P < 0.05$). In contrast, an miR-8080 specific inhibitor increased AR-V7 protein expression, with or without luteolin treatment, and significantly blocked the inhibition of cell viability by luteolin (Figure 5F; $P < 0.05$). These results indicated that AR-V7 is suppressed through translational regulation by miR-8080 in CRPC. We further explored possible signaling pathways regulated by miR-8080 in CRPC. Gene expression changes between 22Rv1 cells transfected with miR-8080 and mock cells were analyzed by RNA sequencing. We detected 405 downregulated genes by miR-8080 in 22Rv1 cells, which were genes related to metabolisms, oxidation–reduction reactions and endoplasmic reticulum (ER) stress (Supplementary Figure S6A and dataset S1, available at *Carcinogenesis* Online). Some AR targeting genes were also downregulated by miR-8080 (Figure 5G). Gene Set Enrichment Analysis indicated a relationship between miR-8080 and ER stress. Gene ontology pathway analysis confirmed signaling pathways associated with ER were significantly downregulated by miR-8080 (Supplementary Figure S6B, dataset S2, available at *Carcinogenesis* Online). *Kyoto* encyclopedia of genes and genomes pathway enrichment analysis also suggested miR-8080 induced upregulation of pathways related to the Unfolded Protein Response, and downregulation of the ER-Associated Degradation (ERAD), may result in the induction of ER stress-related cell death (Dataset S1–3, available at *Carcinogenesis* Online). Of the genes downregulated by miR-8080, 71 genes may have possibility to be direct targets of miR-8080, and did not include ER stress-related genes (Dataset S4, available at *Carcinogenesis* Online). Interestingly, IGF-1R and NKX3.1, which are AR-related genes and strongly related to the proliferation of prostate cancer, including CRPC, were found to be direct targets (Figure 5H). These genes were not only reduced by luteolin but also by miR-8080 induction in 22Rv1 (Figure 5I). These results suggest that miR-8080 indirectly induces ER stress-related cell death, and directly inhibits AR signaling involved in the IGF-1R and NKX3.1.

MiR-8080 enhances the therapeutic efficacy of enzalutamide in CRPC *in vitro* and *in vivo*

The interaction between miR-8080 and AR-V7 stimulated by luteolin raised the question of whether luteolin could improve the therapeutic resistance of enzalutamide against CRPC. Luteolin, when combined with enzalutamide treatment, decreased AR and AR-V7 expression (Figure 6A). Enzalutamide (10 mM) had no effect on the viability of 22Rv1 cells. The combination of luteolin and enzalutamide treatment induced significant growth inhibition in 22Rv1 cells (Figure 6B; $P < 0.001$). Finally, we confirmed the effect of luteolin on the chemotherapeutic efficacy of enzalutamide against CRPC in 22Rv1 tumors in castrated nude mice. Enzalutamide-only treatment did not affect the tumor growth of 22Rv1. However, tumor growth was significantly suppressed by luteolin and, moreover, enzalutamide plus luteolin greatly inhibited tumor growth (Figure 6C and D; $P < 0.01$, $P < 0.001$). Quantitative reverse transcription–polymerase chain reaction indicated that luteolin intake also induced miR-8080 expression in 22Rv1 tumors as compared with vehicle or enzalutamide groups (Figure 6E; $P < 0.05$, $P < 0.001$). AR-V7 mRNA and protein expression were inversely reduced to that of miR-8080 under the same treatment conditions (Figure 6E; $P < 0.001$ for both, Figure 6F).

Discussion

Prostate cancer develops from a hormone sensitive phase to a castration-resistant phase through multiple steps. A decrease in the risk of developing cancer is a basic goal for the chemoprevention of prostate cancer. However, once CRPC has occurred, it is highly lethal due to metastasis and the development of resistance to any treatment. Therefore, new therapeutic strategies addressing CRPC are a key issue. In accordance with a previous study, luteolin has been shown to have inhibitory effects on prostate cancer, both *in vitro* and *ex vivo*. Luteolin suppressed cell proliferation and induced cell-cycle arrest in the G1 phase through the inhibition of IGF-1R signaling in the prostate cancer cell lines, PC-3 and DU-145 (35). The enhancement of apoptosis (35,36) or inhibition of the AR (36,37) is other key contributors to the suppression of prostate cancer by luteolin. In addition, previous studies showed that the intraperitoneal injection of luteolin decreased LNCaP xenograft size in SCID mice or metastatic tumor numbers of PC-3 in nude mice (36,38). In this study, a dietary intake of luteolin clearly suppressed not only the development of

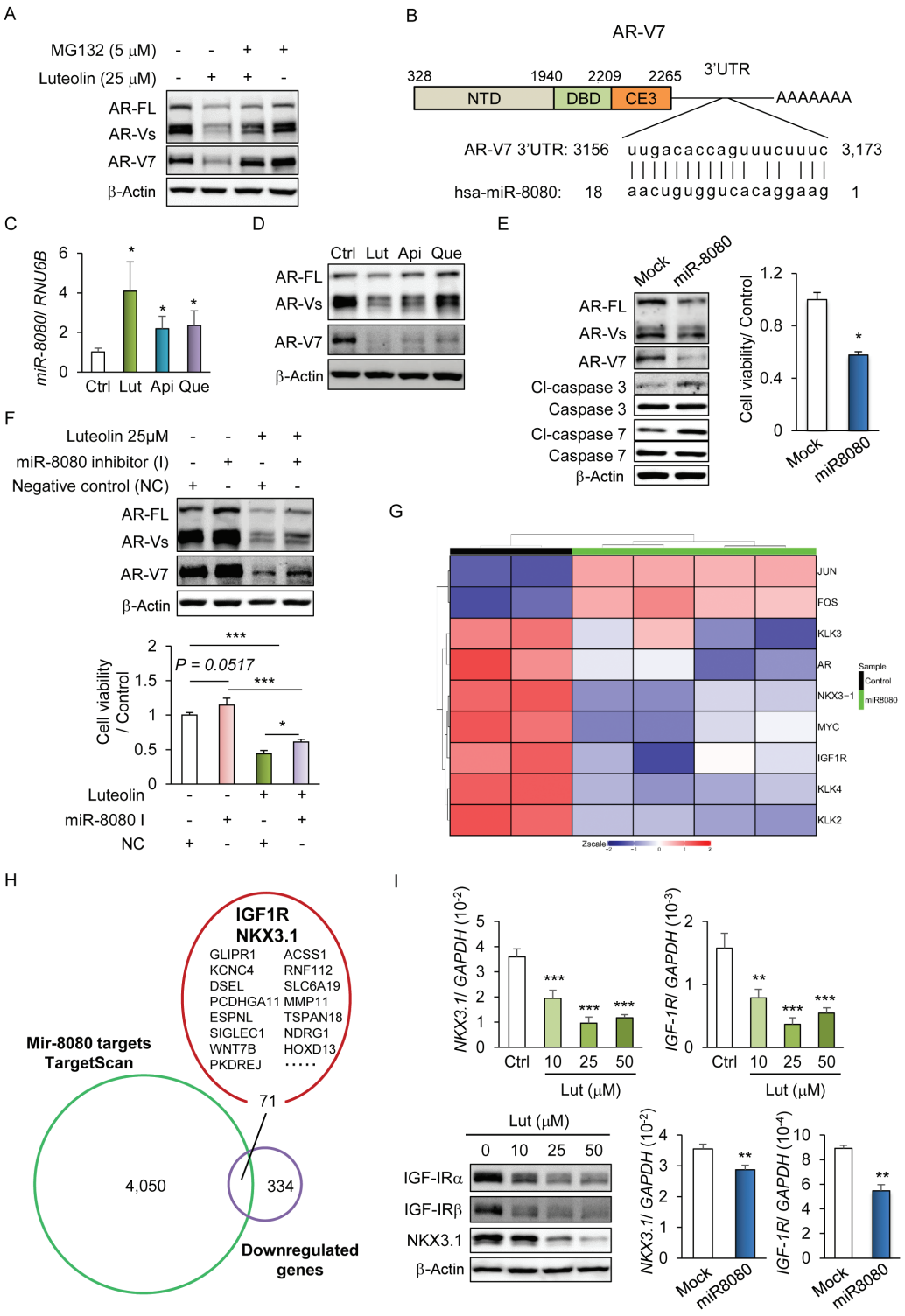

Figure 5. Luteolin inhibits AR-V7 by induction of miR-8080 in 22Rv1 cells. (**A**) Cells (22Rv1) were treated with 25 μM luteolin and/or 5 μM MG132 for 16 h. Western blotting analysis for AR-FL and AR-V7 was carried out. (**B**) *In silico* analysis using the miRbase Sequence Database to detect miRNAs that directly interact with AR-V7. The hsa-miR-8080 can bind the 3′-untranslated region of AR-V7. (**C**) Quantification of miR-8080 expression with luteolin (Lut), apigenin (Api) for 48 h or quercetin (Que) in 22Rv1 cells by quantitative reverse transcription–polymerase chain reaction. Data are presented as mean ± SD, $n = 4$ per group, $^{*}P < 0.05$ statistically significant compared with control group. (**D**) Western blotting analysis for AR-FL and AR-V7 with treatment of Lut, Api or Que for 48 h. (**E**) Effect of miR-8080 transfection on AR-V7 expression and cell proliferation in 22Rv1 cells. The levels of AR-FL, AR-V7, cl-caspases 3 and 7, and caspases 3 and 7 were detected by western blotting. Cell viability is presented as mean ± SD, $n = 4$ per group, $^{*}P < 0.05$ statistically significant compared with mock group. (**F**) Effect of miR-8080 inhibitor on AR-V7 expression and cell proliferation in 22Rv1 cells, with or without luteolin. Levels of AR-FL and AR-V7 protein were detected by western blotting. Cell viability is presented as mean ± SD, $n = 4$ per group, $^{*}P < 0.05$, $^{***}P < 0.001$ statistically significant between the groups shown. (**G**) A heat map of the cluster analysis of AR-related genes. (**H**) Predicted miR-8080 targets searched by TatgetScan (http://www.targetscan.org/vert_72/) and genes downregulated by miR-8080. (**I**) mRNA and protein levels of NKX3.1 and IGF-1R in 22Rv1 cells treated with luteolin or transfected with miR-8080 were analyzed by quantitative reverse transcription–polymerase chain reaction or western blotting. Data are presented as mean ± SD, $n = 4$ per group, $^{**}P < 0.01$, $^{***}P < 0.001$ statistically significant compared with control group.

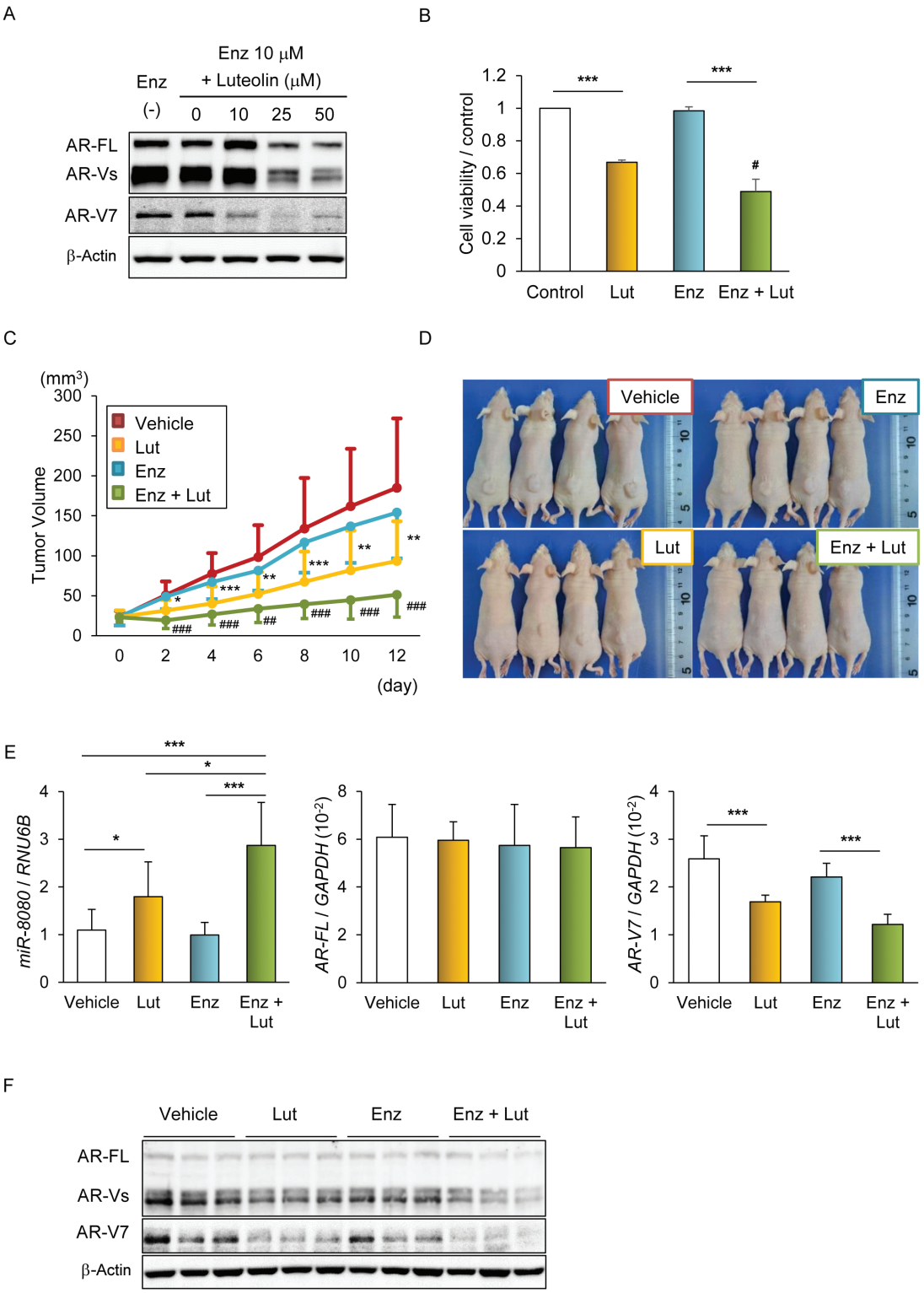

Figure 6. MiR-8080 enhances the chemotherapeutic effect of enzalutamide in 22Rv1 cells both *in vitro* and *ex vivo*. (**A**, **B**) Cells (22Rv1) were treated with enzalutamide (Enz), with or without luteolin (Lut) for 48 h. (A) Western blotting analyses for AR-FL and AR-V7. (B) Cell viability is presented as mean ± SD, $n = 4$ per group, $^{\#}P < 0.05$ statistically significant between Lut and Enz + Lut, and $^{***}P < 0.001$ statistically significant between the groups shown. (**C**–**F**) Effect of luteolin on the chemotherapeutic efficacy of enzalutamide in 22Rv1 xenografts (1.0×10^6 cells) in castrated nude mice. Sixty mice were randomly divided into four groups: vehicle, Lut (luteolin 100 ppm in diet), Enz (enzalutamide 10 mg/kg/day, intraperitoneal injection, 5 times weekly) or Enz + Lut (luteolin 100 ppm + enzalutamide 10 mg/kg/day). (C) Tumor volumes of 22Rv1 xenografts are presented as mean ± SD in each week. $n = 15$ per group, $^{*}P < 0.05$, $^{**}P < 0.01$, $^{***}P < 0.001$ statistically significant between Lut and vehicle groups, $^{\#\#}P < 0.01$, $^{\#\#\#}P < 0.001$ statistically significant between Lut and Enz + Lut group. (D) Gross morphology of subcutaneous 22Rv1 tumors at 2 weeks. (E) Quantitative gene expression of miR-8080, AR-FL and AR-V7 by quantitative reverse transcription–polymerase chain reaction. Data are presented as mean ± SD. $n = 8$ per group, $^{*}P < 0.05$, $^{***}P < 0.001$ statistically significant between groups shown. (F) Western blotting analysis for AR-FL and AR-V7 in 22Rv1 xenografts.

early prostate carcinogenesis in TRAP rats, but also tumor growth of CRPC through the induction of apoptosis without any adverse effects. This is the first report to show an effect of dietary luteolin on prostate carcinogenesis and CRPC. Given that luteolin is used as a chemopreventive agent for humans, an oral intake may be a more natural route for administration.

Oxidative stress is involved in the development of many cancers, including prostate. The production of ROS is mainly regulated by androgens in prostate tissue (39). ROS accumulation can induce gene mutations, alterations of the mitochondrial metabolic pathway, and the activation of AR, resulting in the dysregulation of apoptosis and development of prostate cancer (40). Our data indicate that dietary luteolin suppressed ROS accumulation and induced apoptosis in both TRAP prostate tumors and CRPC tumors of both rat and humans. These findings are consistent with previous reports and indicate that enhancement of apoptosis by protection against ROS is one of the important mechanisms for luteolin as an anticancer agent. An antioxidative effect and increased apoptosis were also observed in CRPC.

MicroRNAs are small endogenous noncoding RNAs that consist of 19–25 nucleotides, and control protein coding genes through mRNA interference (41,42). Posttranscriptional regulation by miRNAs plays an important role in both normal fetal development and cancer progression by controlling cell differentiation, proliferation and apoptosis (43). For example, miRNAs of the miR-34 family are induced by p53 and downregulate their target mRNA in many cancers (44). Specifically, miR-34a and miR-34c are upregulated in prostate cancer cells, and their expression and that of AR protein are inversely correlated in clinical prostate cancer tissues (45). Other miRNAs, miR-30b-3p and miR-30d-5p, regulate both AR and AR-V7 in prostate cancer, and are involved in CRPC cell growth (46). In contrast to the direct interaction of miRNAs and AR, miR-212 indirectly inhibits AR signaling through the downregulation of heterogeneous nuclear ribonucleoprotein H1 in CRPC (47). In this study, miR-8080 was identified as being upregulated by luteolin. MiR-8080 has a target sequence in the 3′-UTR of AR-V7 and therefore could directly interact with AR-V7 but not with AR-FL. However, miR-8080 transfection decreased AR expression and miR-8080 inhibition upregulated AR in 22Rv1 (Figure 5E and F). RNA sequencing analysis indicates IGF-1R and NKX3.1, which are AR-related genes, were directly downregulated by miR-8080. That is why miR-8080 altered AR-FL expression in 22Rv1 cells. In addition, luteolin also induced miRNAs that targeted AR-FL and decreased AR-FL protein expression. Silencing of AR-V7 by specific siRNA induced decreased proliferation in 22Rv1 cells. AR knockdown also induced growth inhibition in 22Rv1 cells, though the effect was less than for AR-V7. These results suggest that the efficacy of miR-8080/AR-V7 therapy against CRPC may be enhanced by a combination of miRNAs targeting AR-FL. As the other possible signaling pathways except AR signaling, miR-8080 changed the expression of genes related to an ER response. Imbalances in ERAD, clearing accumulated misfolded proteins in the ER, and Unfolded Protein Response, activating accumulation of misfolded proteins, are key inducers of ER stress (48). ER stress induces cell death and regulates cancer development including metastasis (48,49). With regard to prostate cancer, androgen treatment promotes ERAD activity by regulating mRNA and protein expression of ERAD components, and may related to prostate tumorigenesis (49). In the present study, genes associated with ERAD were downregulated, and those associated with Unfolded Protein Response were upregulated, resulting in the induction of ER stress by miR-8080 expression in 22Rv1 cells. This suggests that miR-8080 may provide a cell death-sensitive environment by the induction of ER stress via AR-V7 directly or AR-FL indirectly in CRPC.

Novel efficacious therapeutic options for CRPC exist such as enzalutamide or abiraterone. However, most patients are resistant to these drugs owing to the expression of active AR-Vs, such as AR-V7, in the absence of androgen (20,50). CRPC can maintain a dependence on AR signaling, even acquiring resistance to hormonal interventions (20,50). Therefore, AR-V7 is a key protein to consider in any novel strategy of CRPC therapy. The present study indicates that luteolin and its induced expression of miR-8080 improved the chemotherapeutic resistance of enzalutamide against CRPC, both *in vitro* and *in vivo*. These results suggest that a supplemental miR-8080 can be beneficial to the efficacy of enzalutamide. In further studies, we need to explore methodologies on how to deliver active miRNAs to patients with CRPC.

In conclusion, luteolin suppresses both the early stage of prostate carcinogenesis and CRPC via the induction of apoptosis. MiR-8080 induced by luteolin supplementation has an important role in the reduction of AR-V7 protein, resulting in inhibiting tumorigenesis and the enzalutamide resistance of CRPC. Therefore, miR-8080 may be a novel therapeutic target for CRPC.

Supplementary material

Supplementary data are available at *Carcinogenesis* online.

Table S1. Sequence of primers used for quantitative RT–PCR.

Table S2. Body, organ weights and serum hormone levels of TRAP rats treated with luteolin.

Table S3. Incidence of carcinoma and quantitative evaluation of neoplastic lesions in prostates of TRAP rats treated with luteolin.

Table S4. MicroRNAs upregulated by luteolin treatment in 22Rv1.

Dataset S1. Differentially expressed gene analysis of RNA sequence for 22Rv1 cells transfected by miR-8080.

Dataset S2. Gene ontology of the upregulated and downregulated genes by miR-8080.

Dataset S3. KEGG pathway enrichment analysis of the upregulated and downregulated genes by miR-8080.

Dataset S4. MiR-8080 target genes.

Figure S1. Chemopreventive effect of luteolin in prostate carcinogenesis in ventral lobe of transgenic rat for adenocarcinoma of prostate (TRAP) model.

Figure S2. Expression of AR and SV40T in luteolin treated TRAP model.

Figure S3. Expression of redox genes in luteolin treated TRAP model.

Figure S4. Effect of luteolin on cell proliferation in PCai1 with charcoal-stripped fetal bovine serum.

Figure S5. Luteolin, quercetin and apigenin biochemical structures.

Figure S6. Expression of key genes in endoplasmic reticulum is decreased by miR-8080 expression in 22Rv1.

Funding

This work was supported by a Grant-in-Aid for the 3rd Term of a Comprehensive 10-Year Strategy for Cancer Control from the Ministry of Health, Labour and Welfare of Japan to ST; a Grant-in-Aid for Research at Nagoya City University to AN-I and a grant from Ono Pharmaceutical Co., Ltd to ST.

Author contribution statement

AN-I and ST conceived, designed the experiments and supervised the project. AN-I, TN, HK, KI, TE and YN carried out the experiments. AN-I, TN, HK, KI, SS, YY, SI, MO and YT acquired and analyzed the data. AN-I, TN, SS, YY, SI, MO, YT and TY, interpreted

the data, AN-I, TN and ST wrote the paper. All authors discussed the results and contributed to the manuscript.
Conflict of interest statement: None declared.

References

1. Siegel, R.L. *et al.* (2018) Cancer statistics, 2018. *CA. Cancer J. Clin.*, 68, 7–30.
2. Nakai, Y. *et al.* (2007) The dietary charred meat carcinogen 2-amino-1-methyl-6-phenylimidazo[4,5-b]pyridine acts as both a tumor initiator and promoter in the rat ventral prostate. *Cancer Res.*, 67, 1378–1384.
3. Nakai, Y. *et al.* (2013) Inflammation and prostate carcinogenesis. *Int. J. Urol.*, 20, 150–160.
4. Giovannucci, E. *et al.* (1993) A prospective study of dietary fat and risk of prostate cancer. *J. Natl. Cancer Inst.*, 85, 1571–1579.
5. Di Sebastiano, K.M. *et al.* (2014) The role of dietary fat throughout the prostate cancer trajectory. *Nutrients*, 6, 6095–6109.
6. Long, N. *et al.* (2013) Purple corn color inhibition of prostate carcinogenesis by targeting cell growth pathways. *Cancer Sci.*, 104, 298–303.
7. Naiki-Ito, A. *et al.* (2015) Ellagic acid, a component of pomegranate fruit juice, suppresses androgen-dependent prostate carcinogenesis via induction of apoptosis. *Prostate*, 75, 151–160.
8. Suzuki, S. *et al.* (2013) Apocynin, an NADPH oxidase inhibitor, suppresses rat prostate carcinogenesis. *Cancer Sci.*, 104, 1711–1717.
9. Takahashi, S. *et al.* (2009) Suppression of prostate cancer in a transgenic rat model via gamma-tocopherol activation of caspase signaling. *Prostate*, 69, 644–651.
10. López-Lázaro, M. (2009) Distribution and biological activities of the flavonoid luteolin. *Mini Rev. Med. Chem.*, 9, 31–59.
11. Lim, D.Y. *et al.* (2012) Luteolin decreases IGF-II production and downregulates insulin-like growth factor-I receptor signaling in HT-29 human colon cancer cells. *BMC Gastroenterol.*, 12, 9.
12. Osman, N.H. *et al.* (2015) Luteolin supplementation adjacent to aspirin treatment reduced dimethylhydrazine-induced experimental colon carcinogenesis in rats. *Tumour Biol.*, 36, 1179–1190.
13. Pandurangan, A.K. *et al.* (2014) Luteolin inhibits matrix metalloproteinase 9 and 2 in azoxymethane-induced colon carcinogenesis. *Hum. Exp. Toxicol.*, 33, 1176–1185.
14. Sagawa, H. *et al.* (2015) Connexin 32 and luteolin play protective roles in non-alcoholic steatohepatitis development and its related hepatocarcinogenesis in rats. *Carcinogenesis*, 36, 1539–1549.
15. Huggins, C. (1967) Endocrine-induced regression of cancers. *Science*, 156, 1050–1054.
16. de Bono, J.S. *et al.*; COU-AA-301 Investigators. (2011) Abiraterone and increased survival in metastatic prostate cancer. *N. Engl. J. Med.*, 364, 1995–2005.
17. Scher, H.I. *et al.*; AFFIRM Investigators. (2012) Increased survival with enzalutamide in prostate cancer after chemotherapy. *N. Engl. J. Med.*, 367, 1187–1197.
18. Myung, J.K. *et al.* (2013) An androgen receptor N-terminal domain antagonist for treating prostate cancer. *J. Clin. Invest.*, 123, 2948–2960.
19. Yu, Z. *et al.* (2014) Galeterone prevents androgen receptor binding to chromatin and enhances degradation of mutant androgen receptor. *Clin. Cancer Res.*, 20, 4075–4085.
20. Antonarakis, E.S. *et al.* (2014) AR-V7 and resistance to enzalutamide and abiraterone in prostate cancer. *N. Engl. J. Med.*, 371, 1028–1038.
21. Asamoto, M. *et al.* (2001) Prostate carcinomas developing in transgenic rats with SV40 T antigen expression under probasin promoter control are strictly androgen dependent. *Cancer Res.*, 61, 4693–4700.
22. Cho, Y.M. *et al.* (2003) Age-dependent histopathological findings in the prostate of probasin/SV40 T antigen transgenic rats: lack of influence of carcinogen or testosterone treatment. *Cancer Sci.*, 94, 153–157.
23. Hokaiwado, N. *et al.* (2008) Glutathione S-transferase Pi mediates proliferation of androgen-independent prostate cancer cells. *Carcinogenesis*, 29, 1134–1138.
24. Naiki, T. *et al.* (2012) Organ specific Gst-pi expression of the metastatic androgen independent prostate cancer cells in nude mice. *Prostate*, 72, 533–541.
25. Naiki, T. *et al.* (2014) GPX2 overexpression is involved in cell proliferation and prognosis of castration-resistant prostate cancer. *Carcinogenesis*, 35, 1962–1967.
26. Ito, Y. *et al.* (2018) Chemopreventive effects of angiotensin II receptor type 2 agonist on prostate carcinogenesis by the down-regulation of the androgen receptor. *Oncotarget*, 9, 13859–13869.
27. Hu, R. *et al.* (2009) Ligand-independent androgen receptor variants derived from splicing of cryptic exons signify hormone-refractory prostate cancer. *Cancer Res.*, 69, 16–22.
28. Naiki-Ito, A. *et al.* (2007) Gpx2 is an overexpressed gene in rat breast cancers induced by three different chemical carcinogens. *Cancer Res.*, 67, 11353–11358.
29. Naiki, T. *et al.* (2018) GPX2 promotes development of bladder cancer with squamous cell differentiation through the control of apoptosis. *Oncotarget*, 9, 15847–15859.
30. Suzuki, S. *et al.* (2013) Expression of glutathione peroxidase 2 is associated with not only early hepatocarcinogenesis but also late stage metastasis. *Toxicology*, 311, 115–123.
31. Kallio, H.M.L. *et al.* (2018) Constitutively active androgen receptor splice variants AR-V3, AR-V7 and AR-V9 are co-expressed in castration-resistant prostate cancer metastases. *Br. J. Cancer*, 119, 347–356.
32. Kohli, M. *et al.* (2017) Androgen receptor variant AR-V9 is coexpressed with AR-V7 in prostate cancer metastases and predicts abiraterone resistance. *Clin. Cancer Res.*, 23, 4704–4715.
33. Molife, L.R. *et al.* (2010) The insulin-like growth factor-I receptor inhibitor figitumumab (CP-751,871) in combination with docetaxel in patients with advanced solid tumours: results of a phase Ib dose-escalation, open-label study. *Br. J. Cancer*, 103, 332–339.
34. Wang, X. *et al.* (2015) Cabozantinib inhibits abiraterone's upregulation of IGFIR phosphorylation and enhances its anti-prostate cancer activity. *Clin. Cancer Res.*, 21, 5578–5587.
35. Fang, J. *et al.* (2007) Luteolin inhibits insulin-like growth factor 1 receptor signaling in prostate cancer cells. *Carcinogenesis*, 28, 713–723.
36. Chiu, F.L. *et al.* (2008) Downregulation of androgen receptor expression by luteolin causes inhibition of cell proliferation and induction of apoptosis in human prostate cancer cells and xenografts. *Prostate*, 68, 61–71.
37. Tsui, K.H. *et al.* (2012) Upregulation of prostate-derived Ets factor by luteolin causes inhibition of cell proliferation and cell invasion in prostate carcinoma cells. *Int. J. Cancer*, 130, 2812–2823.
38. Zhou, Q. *et al.* (2009) Luteolin inhibits invasion of prostate cancer PC3 cells through E-cadherin. *Mol. Cancer Ther.*, 8, 1684–1691.
39. Tam, N.N. *et al.* (2003) Androgenic regulation of oxidative stress in the rat prostate: involvement of NAD(P)H oxidases and antioxidant defense machinery during prostatic involution and regrowth. *Am. J. Pathol.*, 163, 2513–2522.
40. Dakubo, G.D. *et al.* (2006) Altered metabolism and mitochondrial genome in prostate cancer. *J. Clin. Pathol.*, 59, 10–16.
41. Kim, V.N. *et al.* (2006) Genomics of microRNA. *Trends Genet.*, 22, 165–173.
42. Ma, C. *et al.* (2009) MicroRNAs—powerful repression comes from small RNAs. *Sci. China C: Life Sci.*, 52, 323–330.
43. Su, Z. *et al.* (2015) MicroRNAs in apoptosis, autophagy and necroptosis. *Oncotarget*, 6, 8474–8490.
44. Rokavec, M. *et al.* (2014) The p53/miR-34 axis in development and disease. *J. Mol. Cell Biol.*, 6, 214–230.
45. Östling, P. *et al.* (2011) Systematic analysis of microRNAs targeting the androgen receptor in prostate cancer cells. *Cancer Res.*, 71, 1956–1967.
46. Kumar, B. *et al.* (2016) Identification of miR-30b-3p and miR-30d-5p as direct regulators of androgen receptor signaling in prostate cancer by complementary functional microRNA library screening. *Oncotarget*, 7, 72593–72607.
47. Yang, Y. *et al.* (2016) Dysregulation of miR-212 promotes castration resistance through hnRNPH1-mediated regulation of AR and AR-V7: implications for racial disparity of prostate cancer. *Clin. Cancer Res.*, 22, 1744–1756.
48. Jeon, Y.J. *et al.* (2018) miRNA-mediated TUSC3 deficiency enhances UPR and ERAD to promote metastatic potential of NSCLC. *Nat. Commun.*, 9, 5110.
49. Erzurumlu, Y. *et al.* (2017) Androgen mediated regulation of endoplasmic reticulum-associated degradation and its effects on prostate cancer. *Sci. Rep.*, 7, 40719.
50. Antonarakis, E.S. *et al.* (2017) Clinical significance of androgen receptor splice Variant-7 mRNA detection in circulating tumor cells of men with metastatic castration-resistant prostate cancer treated with first- and second-line abiraterone and enzalutamide. *J. Clin. Oncol.*, 35, 2149–2156.